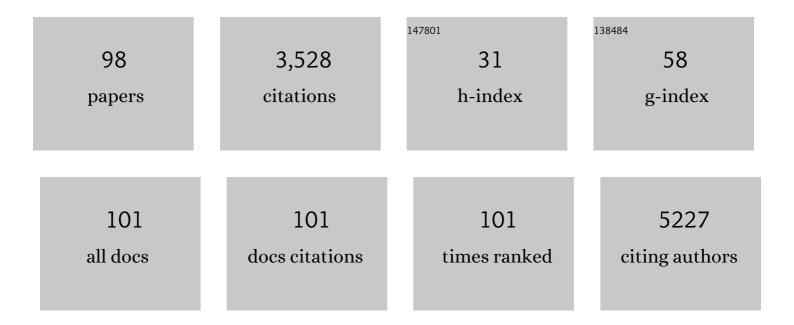
Cécile Hébert

List of Publications by Year in descending order

Source: https://exaly.com/author-pdf/5787061/publications.pdf Version: 2024-02-01



#	Article	IF	CITATIONS
1	3D reconstruction of curvilinear structures with stereo matching deep convolutional neural networks. Ultramicroscopy, 2022, 234, 113460.	1.9	5
2	Investigating Magma Ocean Solidification on Earth Through Laserâ€Heated Diamond Anvil Cell Experiments. Geophysical Research Letters, 2021, 48, e2021GL092446.	4.0	12
3	3D Ordering at the Liquid–Solid Polar Interface of Nanowires. Advanced Materials, 2020, 32, e2001030.	21.0	10
4	Machine Learning on STEM-EDS Data for Quantifying Overlapping Deep-Mantle Rock Assemblages. Microscopy and Microanalysis, 2020, 26, 1878-1880.	0.4	1
5	Triplet grain growth in a-texture polycrystalline ZnO thin films. Acta Materialia, 2020, 199, 523-529.	7.9	0
6	MOOCS: A New Way of Teaching Transmission Electron Microscopy. Microscopy and Microanalysis, 2019, 25, 2270-2271.	0.4	0
7	Quantifying competitive grain overgrowth in polycrystalline ZnO thin films. Acta Materialia, 2019, 173, 74-86.	7.9	5
8	Insights into image contrast from dislocations in ADF-STEM. Ultramicroscopy, 2019, 200, 139-148.	1.9	18
9	Evolution of the properties of helium nanobubbles during <i>in situ</i> annealing probed by spectrum imaging in the transmission electron microscope. Physical Review B, 2018, 97, .	3.2	13
10	A large planetary body inferred from diamond inclusions in a ureilite meteorite. Nature Communications, 2018, 9, 1327.	12.8	56
11	Three-dimensional scanning transmission electron microscopy of dislocation loops in tungsten. Micron, 2018, 113, 24-33.	2.2	29
12	Stereo-vision three-dimensional reconstruction of curvilinear structures imaged with a TEM. Ultramicroscopy, 2018, 184, 116-124.	1.9	15
13	Direct Imaging of Dopant Distribution in Polycrystalline ZnO Films. ACS Applied Materials & Interfaces, 2017, 9, 7241-7248.	8.0	7
14	Zinc blende–wurtzite polytypism in nanocrystalline ZnO films. Acta Materialia, 2017, 130, 240-248.	7.9	12
15	Combining in-Situ SEM with High Sensitivity Analytical TEM for Understanding the Degradation of Metallic Interconnects in SOFC. Microscopy and Microanalysis, 2017, 23, 2060-2061.	0.4	1
16	Electron Energy Loss Near Edge Structures as a Tool to Elucidate Natural and Artificial Minerals Structures. Microscopy and Microanalysis, 2017, 23, 2154-2155.	0.4	1
17	Computer Vision Techniques Applied to the Reconstruction of the 3-D Structure Dislocations. Microscopy and Microanalysis, 2017, 23, 102-103.	0.4	0
18	Tilt-less 3-D electron imaging and reconstruction of complex curvilinear structures. Scientific Reports, 2017, 7, 10630.	3.3	19

#	Article	IF	CITATIONS
19	In-Situ Observation of Co-Ce Coated Metallic Interconnect Oxidation Combined with High-Resolution Post Exposure Analysis. ECS Transactions, 2017, 78, 1615-1632.	0.5	5
20	Properties of helium bubbles in covalent systems at the nanoscale: A combined numerical and experimental study. Physical Review B, 2017, 96, .	3.2	16
21	EFTEM Pre- and Post-Irradiation sp 2 to sp 3 R-Ratio Measurements Of SiC/SiC Pyrolytic Carbon Interphases. Microscopy and Microanalysis, 2016, 22, 1466-1467.	0.4	1
22	Energy-filtered environmental transmission electron microscopy for the assessment of solid–gas reactions at elevated temperature: NiO/YSZ–H2 as a case study. Ultramicroscopy, 2016, 169, 11-21.	1.9	5
23	Strain-driven oxygen deficiency in multiferroic <mml:math xmlns:mml="http://www.w3.org/1998/Math/MathML"><mml:msub><mml:mi>SrMnO</mml:mi><mml:mn>3films. Physical Review B, 2016, 94, .</mml:mn></mml:msub></mml:math 	ml 312 1> <td>mnslemsub><!--</td--></td>	mn sle msub> </td
24	Spin and valence dependence of iron partitioning in Earth's deep mantle. Proceedings of the National Academy of Sciences of the United States of America, 2016, 113, 11127-11130.	7.1	45
25	A TEM study of Ni interfaces formed during activation of SOFC anodes in H2: Influence of grain boundary symmetry and segregation of impurities. Acta Materialia, 2016, 103, 442-447.	7.9	12
26	Toward Knowledgeâ€Based Grainâ€Boundary Engineering of Transparent Alumina Combining Advanced <scp>TEM</scp> and Atomistic Modeling. Journal of the American Ceramic Society, 2015, 98, 1959-1964.	3.8	9
27	Microstructural stability of ODS steels in cyclic loading. Fatigue and Fracture of Engineering Materials and Structures, 2015, 38, 936-947.	3.4	22
28	Direct visualization of dispersed lipid bicontinuous cubic phases by cryo-electron tomography. Nature Communications, 2015, 6, 8915.	12.8	116
29	Direct Evidence of Surface Reduction in Monoclinic BiVO ₄ . Chemistry of Materials, 2015, 27, 3593-3600.	6.7	78
30	Height-resolved quantification of microstructure and texture in polycrystalline thin films using TEM orientation mapping. Ultramicroscopy, 2015, 159, 112-123.	1.9	13
31	Increasing Polycrystalline Zinc Oxide Grain Size by Control of Film Preferential Orientation. Crystal Growth and Design, 2015, 15, 5886-5891.	3.0	19
32	Gentle quantitative measurement of helium density in nanobubbles in silicon by spectrum imaging. Micron, 2015, 77, 57-65.	2.2	16
33	Segregation of anion (Clâ^') impurities at transparent polycrystalline α-alumina interfaces. Journal of the European Ceramic Society, 2014, 34, 3037-3045.	5.7	4
34	Oxidation mechanism of nickel particles studied in an environmental transmission electron microscope. Acta Materialia, 2014, 67, 362-372.	7.9	47
35	Measurements of local chemistry and structure in Ni(O)–YSZ composites during reduction using energy-filtered environmental TEM. Chemical Communications, 2014, 50, 1808.	4.1	9
36	Enhanced Quantification for 3D Energy Dispersive Spectrometry: Going Beyond the Limitation of Large Volume of X-Ray Emission. Microscopy and Microanalysis, 2014, 20, 1544-1555.	0.4	6

#	Article	IF	CITATIONS
37	Time-Resolved X-Ray Microtomography Observation of Intermetallic Formation Between Solid Fe and Liquid Al. Metallurgical and Materials Transactions A: Physical Metallurgy and Materials Science, 2013, 44, 4119-4123.	2.2	23
38	Corona protein composition and cytotoxicity evaluation of ultra-small zeolites synthesized from template free precursor suspensions. Toxicology Research, 2013, 2, 270.	2.1	41
39	Reduction of nickel oxide particles by hydrogen studied in an environmental TEM. Journal of Materials Science, 2013, 48, 2893-2907.	3.7	122
40	Dynamic structure factors of Cu, Ag, and Au: Comparative study from first principles. Physical Review B, 2013, 88, .	3.2	31
41	Multivariate statistical analysis as a tool for the segmentation of 3D spectral data. Micron, 2013, 52-53, 49-56.	2.2	86
42	Nanoprecipitates in single-crystal molybdenum-alloy nanopillars detected by TEM and atom probe tomography. Scripta Materialia, 2013, 69, 41-44.	5.2	2
43	Advanced materials characterization and modeling using synchrotron, neutron, TEM, and novel micro-mechanical techniques—A European effort to accelerate fusion materials development. Journal of Nuclear Materials, 2013, 442, S834-S845.	2.7	10
44	Imaging of high- <mml:math <br="" xmlns:mml="http://www.w3.org/1998/Math/MathML">display="inline"><mml:mi>Q</mml:mi></mml:math> cavity optical modes by electron energy-loss microscopy. Physical Review B, 2013, 87, .	3.2	11
45	Identifying champion nanostructures for solar water-splitting. Nature Materials, 2013, 12, 842-849.	27.5	527
46	Quantitative imaging of flux vortices in the type-II superconductor MgB <mml:math xmlns:mml="http://www.w3.org/1998/Math/MathML" display="inline"><mml:msub><mml:mrow /><mml:mn>2</mml:mn></mml:mrow </mml:msub>using cryo-Lorentz transmission electron microscopy. Physical Review B, 2013, 88, .</mml:math 	3.2	10
47	Slip in directionally solidified Mo-alloy micropillars – Part I: Nominally dislocation-free pillars. Acta Materialia, 2012, 60, 4604-4613.	7.9	13
48	A perspective on novel sources of ultrashort electron and X-ray pulses. Chemical Physics, 2012, 392, 1-9.	1.9	51
49	Statistical analysis of oxides particles in ODS ferritic steel using advanced electron microscopy. Journal of Nuclear Materials, 2012, 422, 131-136.	2.7	13
50	Silicon Filaments in Silicon Oxide for Nextâ€Generation Photovoltaics. Advanced Materials, 2012, 24, 1182-1186.	21.0	118
51	Capturing EELS in the reciprocal space. EPJ Applied Physics, 2011, 54, 33510.	0.7	3
52	Electronic Interactions between "Pea―and "Pod― The Case of Oligothiophenes Encapsulated in Carbon Nanotubes. Small, 2011, 7, 1807-1815.	10.0	37
53	Encapsulation of Conjugated Oligomers in Singleâ€Walled Carbon Nanotubes: Towards Nanohybrids for Photonic Devices. Advanced Materials, 2010, 22, 1635-1639.	21.0	112
54	Theoretical analysis of the momentum-dependent loss function of bulk Ag. Ultramicroscopy, 2010, 110, 1081-1086.	1.9	20

#	Article	IF	CITATIONS
55	Tuning the photophysical properties of soluble single-wall carbon nanotube derivatives by co-functionalization with organic molecules. Carbon, 2009, 47, 1264-1269.	10.3	18
56	Imaging of GaAs Nanowire Using Combined Aberration-corrected TEM/STEM and Exit Wave Restoration. Microscopy and Microanalysis, 2009, 15, 138-139.	0.4	1
57	Investigation of 6T@SWCNT by Cs-Corrected Transmission Electron Microscopy. Microscopy and Microanalysis, 2009, 15, 1334-1335.	0.4	0
58	Magnetic circular dichroism in EELS: Towards 10nm resolution. Ultramicroscopy, 2008, 108, 433-438.	1.9	59
59	Optimal aperture sizes and positions for EMCD experiments. Ultramicroscopy, 2008, 108, 865-872.	1.9	31
60	Magnetic circular dichroism in electron energy loss spectrometry. Ultramicroscopy, 2008, 108, 277-284.	1.9	30
61	Energy-loss magnetic chiral dichroism (EMCD): Magnetic chiral dichroism in the electron microscope. Journal of Materials Research, 2008, 23, 2582-2590.	2.6	32
62	TEM and SEM Investigation on Oxidised Ge-based Clathrates. Microscopy and Microanalysis, 2008, 14, 1142-1143.	0.4	0
63	Energy loss magnetic chiral dichroism: A new technique for the study of magnetic properties in the electron microscope (invited). Journal of Applied Physics, 2008, 103, .	2.5	34
64	Magnetic Circular Dichroism in Electron Microscopy. Acta Physica Polonica A, 2008, 113, 599-644.	0.5	9
65	EMCD: Magnetic Chiral Dichroism in the Electron Microscope. Materials Research Society Symposia Proceedings, 2007, 1026, 1.	0.1	0
66	Nanocarbon as Robust Catalyst: Mechanistic Insight into Carbonâ€Mediated Catalysis. Angewandte Chemie - International Edition, 2007, 46, 7319-7323.	13.8	226
67	Practical aspects of running the WIEN2k code for electron spectroscopy. Micron, 2007, 38, 12-28.	2.2	130
68	Lifetime of Hot Electrons in Metals Retrived From Low Loss EELS. Microscopy and Microanalysis, 2006, 12, 1168-1169.	0.4	1
69	Numerical Aspects of Valence Electron Energy Loss Spectrometry. Microscopy and Microanalysis, 2006, 12, 1180-1181.	0.4	Ο
70	Observation of Magnetic Circular Dichroism in the Electron Microscope. Microscopy and Microanalysis, 2006, 12, 960-961.	0.4	1
71	Electron energy-loss spectrometry for metals: some thoughts beyond microanalysis. International Journal of Materials Research, 2006, 97, 920-927.	0.3	1
72	Detection of magnetic circular dichroism using a transmission electron microscope. Nature, 2006, 441, 486-488.	27.8	331

#	Article	IF	CITATIONS
73	ELNES at magic angle conditions. Ultramicroscopy, 2006, 106, 1139-1143.	1.9	38
74	Experimental and theoretical determination of low electron energy loss spectra of Ag and Ru. Ultramicroscopy, 2006, 106, 1115-1119.	1.9	5
75	Short note on parallel illumination in the TEM. Ultramicroscopy, 2006, 106, 1144-1149.	1.9	7
76	Electron energy-loss spectroscopy investigations of the electron density in ErMn2and ErMn2D2compounds. Journal of Physics Condensed Matter, 2005, 17, 3657-3664.	1.8	1
77	Anisotropic relativistic cross sections for inelastic electron scattering, and the magic angle. Physical Review B, 2005, 72, .	3.2	63
78	Electron energy loss-near edge structure as a fingerprint for identifying chromium nitrides. Solid State Communications, 2004, 130, 209-213.	1.9	33
79	Comment on "Experimental and theoretical evidence for the magic angle in transmission electron energy loss spectroscopy―by H. Daniels, A. Brown, A. Scott, T. Nichells, B. Rand and R. Brydson. Ultramicroscopy, 2004, 101, 271-273.	1.9	9
80	Thickness Dependent Loss Function of Si with 0.14 eV Energy Resolution. Advanced Engineering Materials, 2004, 6, 826-828.	3.5	4
81	Investigation of hexagonal and cubic GaN by high-resolution electron energy-loss spectroscopy and density functional theory. Ultramicroscopy, 2004, 98, 249-257.	1.9	35
82	The magic angle: a solved mystery. Ultramicroscopy, 2004, 102, 61-66.	1.9	56
83	Energy-loss Near-edge Structure (ELNES) of Hexagonal and Cubic GaN. Microscopy and Microanalysis, 2004, 10, 884-885.	0.4	1
84	Observation of Circular Dichroism in the TEM. Microscopy and Microanalysis, 2004, 10, 836-837.	0.4	0
85	A proposal for dichroic experiments in the electron microscope. Ultramicroscopy, 2003, 96, 463-468.	1.9	85
86	Improvement of energy loss near edge structure calculation using Wien2k. Micron, 2003, 34, 219-225.	2.2	64
87	Anisotropy and collection angle dependence of the oxygen K ELNES in V2O5: a band-structure calculation study. Micron, 2003, 34, 227-233.	2.2	20
88	High resolution EELS using monochromator and high performance spectrometer: comparison of V2O5 ELNES with NEXAFS and band structure calculations. Micron, 2003, 34, 235-238.	2.2	41
89	Ionization edges: Some underlying physics and their use in electron microscopy. Advances in Imaging and Electron Physics, 2002, , 413-450.	0.2	3
90	Density Functional Theory as a Tool for the Electron Microscopist. Microscopy and Microanalysis, 2002, 8, 1594-1595.	0.4	1

#	Article	IF	CITATIONS
91	Comparison of ELNES and NEXAFS of vanadium oxide V2O5 with different spectral resolution. Microscopy and Microanalysis, 2002, 8, 602-603.	0.4	0
92	Localization of Low Energy Losses and the Mixed Dynamic Form Factor. Microscopy and Microanalysis, 2002, 8, 636-637.	0.4	1
93	The separation of surface and bulk contributions in ELNES spectra. Ultramicroscopy, 2002, 93, 91-97.	1.9	3
94	Oxygen K-edge in vanadium oxides: simulations and experiments. European Physical Journal B, 2002, 28, 407-414.	1.5	84
95	Partial core hole screening in the Cu L 3 edge. European Physical Journal B, 2001, 21, 363-367.	1.5	51
96	Orientation dependence of ionization edges in EELS. Ultramicroscopy, 2001, 86, 343-353.	1.9	25
97	Electron energy-loss spectroscopy fine structure of the Cu L2,3ionization edge in substitutional Cu-Ni alloys. Journal of Physics Condensed Matter, 2001, 13, 3791-3803.	1.8	9
98	The orientation-dependent simulation of ELNES. Ultramicroscopy, 2000, 83, 9-16.	1.9	70